Flux growth and spectroscopic studies of LiBaB$_9$O$_{15}$ single crystal

**Shujuan Han · Jiyang Wang · Jing Li ·
Yongjie Guo · Yongzheng Wang · Lanling Zhao ·
R. I. Boughton**

Abstract Single crystal of LiBaB$_9$O$_{15}$ for the first time has been grown from a Li$_2$Mo$_3$O$_{10}$ flux by the top-seeded growth method. Details on the preparation and growth procedures are discussed. The phase structure of the as-grown crystal was determined by X-ray powder diffraction (XRD). The frequencies of the vibrational modes of the crystal were obtained from Infrared and Raman spectrum measurements. The results show that the obtained crystal is well-crystallized and indexed as a trigonal crystal system with lattice parameters of a = b=10.95053 Å, c = 16.88215 Å, and V = 1753.19 Å^3. The observed frequencies were assigned on the basis of the BO$_3$ and BO$_4$ vibrations, and correlations with previous data reported for the similar compounds. On the basis of the XRD data and interfacial angle measurements, the as-grown crystal was found to be bounded by the (110), (113), and (101) planes. The seed crystal used for producing the crystal was oriented along the [100] direction.

Introduction

Recently, inorganic borates have been a focus of research because of their applications to different branches of science and technology. After much research effort, many excellent borate crystals have been obtained, such as LiB$_3$O$_5$ (LBO), CBO, β–BaB$_2$O$_4$ (BBO), etc. These

S. Han · J. Wang (✉) · J. Li · Y. Guo · Y. Wang · L. Zhao
State Key Laboratory of Crystal Materials, Shandong University,
Jinan 250100, People's Republic of China
e-mail: jywang@sdu.edu.cn

R. I. Boughton
Department of Physics and Astronomy, Bowling Green State
University, Bowling Green, OH 43403, USA

successes have sparked considerable interest in the search for promising new compounds in ternary systems [1–7].
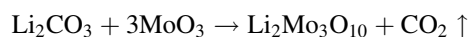
The M$_2$O–RO–B$_2$O$_3$ ternary system (where $M =$ alkaline element, $R =$ alkaline earth element) has attracted much attention in recent years, due to the good nonlinear optical properties of BBO [8] and LBO [9]. LiBaB$_9$O$_{15}$ is one of the materials in this system. LiBaB$_9$O$_{15}$ single crystals were first prepared by Penin et al. [10] using the process of cooling the stoichiometric melt. They found that LiBaB$_9$O$_{15}$ melts congruently at 1050 °C. Nanocrystalline samples of LiBaB$_9$O$_{15}$ were synthesized by Pushcharovsky et al. [11] using a hydrothermal system. However, up to now, only the crystal structure and the thermal properties have been reported, and no satisfactory large-sized crystals have as yet been grown by the flux method.

In this article, the authors report on the details of LiBaB$_9$O$_{15}$ crystal growth for the first time from a Li$_2$Mo$_3$O$_{10}$ flux using the top-seeded solution growth (TSSG) method. Characterization of some properties of the as-grown crystal is reported.

Experimental procedure

Crystal growth

For the first time, single crystal LiBaB$_9$O$_{15}$ was grown at a temperature well below its melting point from a flux melt based on Li$_2$Mo$_3$O$_{10}$, which was obtained using Li$_2$CO$_3$ and MoO$_3$ in stoichiometric proportion. The flux was synthesized according to the following reaction:

$$Li_2CO_3 + 3MoO_3 \rightarrow Li_2Mo_3O_{10} + CO_2 \uparrow$$

The crystal growth experiment was performed in a vertical electric furnace controlled by an FP21 digital

microprocessor temperature programmer-controller (Programmable PID regulator, Island Power Company, Japan) in air. The temperature was measured using a thermocouple. The raw materials were the 4N pure reagents namely Li_2CO_3, $BaCO_3$, and MoO_3 and the analytically pure reagent namely H_3BO_3 (Shanghai Chemical Reagent Co., Ltd., Sinopharm).

Preparation of the seed

The starting materials, Li_2CO_3, $BaCO_3$, H_3BO_3, and MoO_3, in a molar ratio of 5:2:3:1:12, were completely mixed and put into a platinum crucible with dimensions of 70 mm in diameter and 80 mm in height. The platinum crucible was covered with a lid and placed in the center of a vertical, programmable temperature furnace. A platinum wire attached to an alumina shaft was used to initiate crystallization in order to obtain seeds. The mixture was heated from room temperature up to 1000 °C at a rate of 100 °C/h and held at this temperature for 50 h to mix it as homogeneously as possible. After heating, the temperature was lowered to 860 °C at a rate of 50 °C/h. A platinum wire was then slowly inserted into the furnace and dipped into the melt. Subsequently, the temperature was lowered to 730 °C at a rate of 1 °C/h. During the cooling process, some crystals were formed on the platinum wire (see Fig. 1a). The crystals obtained were chemically stable and not hygroscopic. In order to obtain a crystal that was suitable (transparent, no cracks, and few inclusions) to be the seed for crystal growth, the process was repeated until a good seed was obtained.

Top-seeded solution growth (TSSG)

The TSSG method was adopted for crystal growth after the seed was prepared. A crucible with dimensions of 70 mm in diameter and 80 mm in height containing the raw materials was put into the furnace and heated to 1000 °C at a rate of 100 °C/h. It was held at this temperature for 30 h. After that, the saturation temperature of the solution was measured exactly by using the seed-tentative method. The test seed was monitored and the solution temperature was adjusted in response to the observed changes of the seed until the saturation temperature was established [12, 13]. At several degrees above the saturation temperature, the seed was slowly inserted into the surface of the melt. The temperature was held stable for 1 h and then lowered to the saturation temperature after half an hour. The temperature was then continuously lowered at a rate of 0.5 °C/day, and the growing crystal was rotated at a rate of 30 rpm. After growth was completed, the crystal was drawn out of the melt and kept above the surface of the solution while the furnace was cooled slowly to room temperature to avoid thermal shock. Finally, the Li-BaB_9O_{15} single crystal shown in Fig. 1b was obtained.

X-ray powder diffraction analysis

X-ray powder diffraction (XRD) was used to determine the lattice structure and lattice parameters of the as-grown crystal at room temperature. The crystal was ground into powder form for examination. XRD data were recorded on a Japan Burker D8/advance X-ray diffractometer system with graphite monochromatized Cu Kα irradiation ($\lambda = 0.15418$ nm), together with a diffractometer scan step size of $2\theta = 0.02°$, and dwell time of 2 s/step, over a 2θ range of 10–80°.

Spectroscopic studies of $LiBaB_9O_{15}$ single crystal

FTIR spectrum measurement

The FTIR spectrum was measured using (NEXUS670) FTIR Spectrophotometer over the range of 4000–650 cm^{-1} using a KBr reference pellet at room temperature.
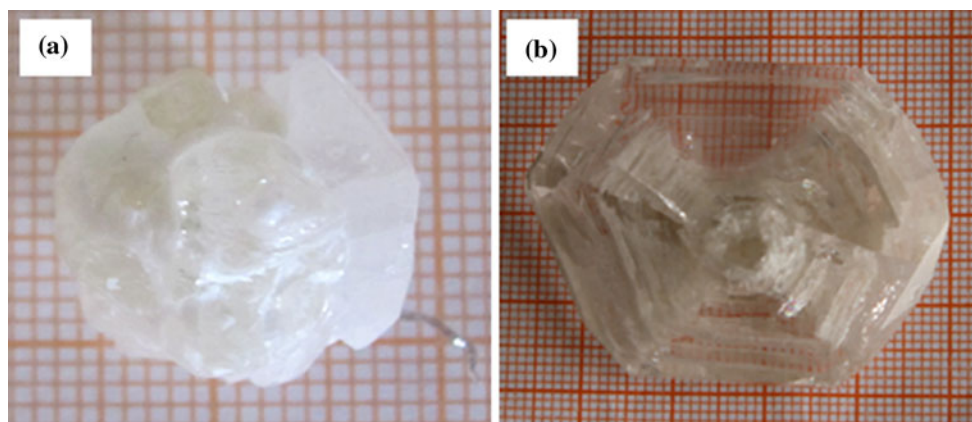
Fig. 1 Photograph of the as-grown $LiBaB_9O_{15}$ crystal

Raman spectrum measurement

The Raman spectrum was collected by a JASCONRS-1000DT micro-Raman spectrophotomer using two scans from 4000 to 100 cm^{-1} with a spectral resolution of 2 cm^{-1}.

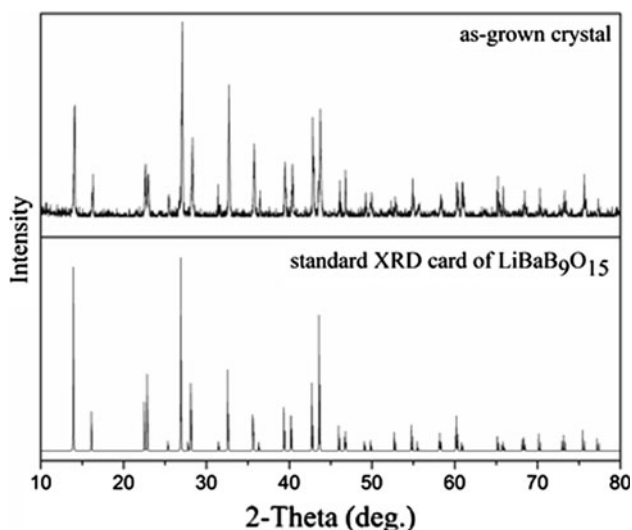## Results and discussion

Flux growth and characteristics of single crystal LiBaB$_9$O$_{15}$

The flux growth technique is especially preferable because it readily allows crystal growth at a temperature well below the melting point of the solute. In addition, crystals grown from the flux have regular morphology. The seed crystal orientation has an effect on the morphology of the crystal. Figure 1b shows the LiBaB$_9$O$_{15}$ crystal with dimensions of $16 \times 35 \times 47$ mm^3 grown with the seed oriented along [100]. On the basis of the XRD data and interfacial angle measurements, the crystal was found to be bounded by the (110), (113), and (101) planes.

Phase identification of the crystal

The XRD pattern of the as-grown crystal is shown in Fig. 2. X-ray analysis shows that as-grown crystal is LiBaB$_9$O$_{15}$. All of the peaks in Fig. 2 can be indexed in accordance with the standard JCPDS Card File 47-341 for LiBaB$_9$O$_{15}$. No additional peaks are found, which confirms that the as-grown crystal is well-crystallized. The lattice parameters were calculated using the program TOPASS from the observed 2θ values (see Table 1). All the results

Table 1 Lattice parameters of LiBaB$_9$O$_{15}$ crystal

Reference	a (Å)	b (Å)	c (Å)	V (Å^3)
[11]	10.982(2)	10.982(2)	17.067(3)	1782.6(5)
This study	10.95053	10.95053	16.88215	1753.19

are in agreement with the report of Pushcharovsky et al. [11].

IR and Raman spectra analysis

Figure 3 shows the IR spectrum of the as-grown LiBaB$_9$O$_{15}$ crystal. The vibrational modes of the borate network are active mainly in three infrared spectral regions: 1500–1200 cm^{-1} (B–O stretching of the triangular BO$_3$ units), 1200–850 cm^{-1} (B–O stretching of the tetrahedral BO$_4$ units), and 800–600 cm^{-1} (bending vibrations of various borate segments) [14]. Most of the vibrational modes and frequencies observed in similar compounds were examined [15–17]. The absorption bands observed in the regions 1470–1243 cm^{-1} are attributed to the B–O asymmetrical stretching vibration of the BO$_3$ unit. The strong absorption bands around 1105, 994, and 906 cm^{-1} arise from the B–O asymmetrical stretching vibration of the BO$_4$ unit. The band observed at around 848 cm^{-1} is related to the B–O symmetric stretching vibration of the tetrahedral BO$_4$ units. The peaks between 790 and 690 cm^{-1} characterize bending modes of the triangular BO$_3$ and tetrahedral BO$_4$ units.

Figure 4 shows the Raman spectrum of the as-grown LiBaB$_9$O$_{15}$ crystal, which confirms the structure proposed by the FT–IR results. The Raman frequencies were assigned on the basis of correlations with previous data reported for other similar compounds [17–19]. The

Fig. 2 X-ray powder diffraction pattern of LiBaB$_9$O$_{15}$ crystal
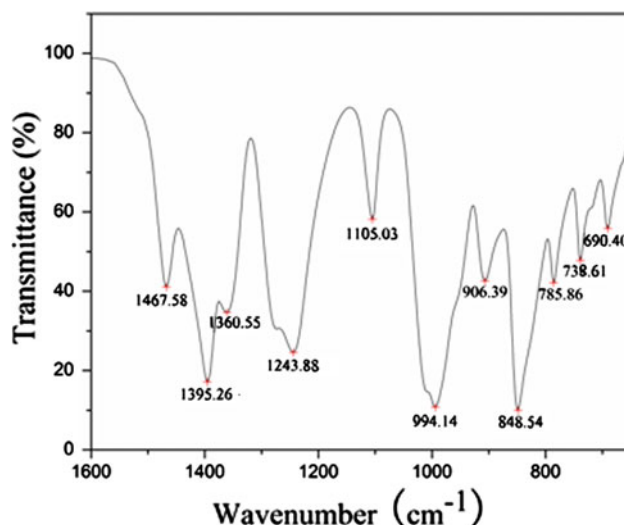
Fig. 3 IR spectrum of LiBaB$_9$O$_{15}$ crystal
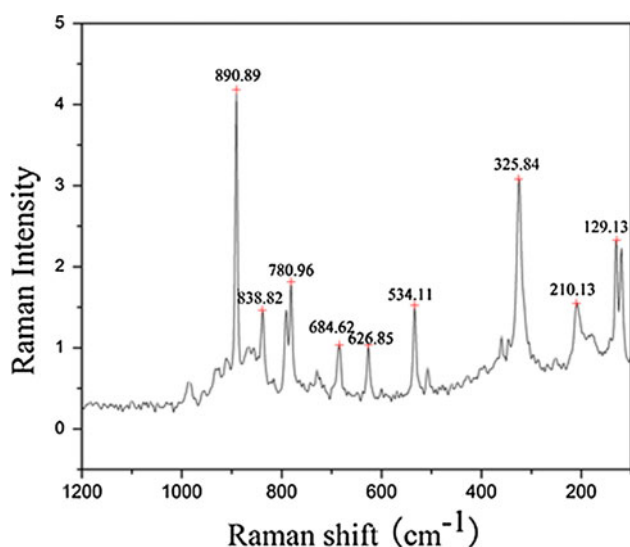
Fig. 4 Raman spectrum of LiBaB$_9$O$_{15}$ crystal

vibrational bands at about 890 and 838 cm^{-1}, respectively are assigned to the B–O asymmetric and symmetric stretching vibration of tetrahedral BO$_4$ units. The bands between 780 and 626 cm^{-1} characterize the B–O bending modes of the triangular BO$_3$ units. The band at about 534 cm^{-1} is related to the B–O symmetrical stretching vibration of the BO$_4$ units. The peak observed at around 325 cm^{-1} arises from the translational motions of the BO$_3$ and BO$_4$ groups, while the vibrations of the BO$_3$ and BO$_4$ groups occur below 250 cm^{-1}.

Conclusions

To summarize, a large LiBaB$_9$O$_{15}$ single crystal has for the first time been successfully grown by the TSSG method. XRD results show that the as-grown crystal is well-crystallized and indexed to the trigonal system. The morphology of the crystal depends strongly on the seed crystal orientation. In future study, the authors expect to grow high quality crystals using this technique.

References

1. Bubnova RS, Krivovichev SV, Filatov SK, Egorysheva AV, Kargin YF (2007) J Solid State Chem 180:596–603
2. Li T, Chen ZP, Su YL, Su L, Zhang JC (2009) J Mater Sci 44:6149–6154. doi:10.1007/s10853-009-3850-8
3. Hu ZG, Yoshimura M, Mori Y, Sasaki T (2005) J Cryst Growth 275:232–239
4. Li ZH, Zhang DM, Yang FX (2009) J Mater Sci 44:2435–2443. doi:10.1007/s10853-009-3316-z
5. Karnal AK, Bhaumik I, Ganesamoorthy S, Bhatt R, Saxena A, Wadhawan VK, Bhat HL (2007) Mater Lett 61:600–604
6. Vengala RB, Buddhudu S (2007) J Mater Sci 43:233–236. doi:10.1007/s10853-007-1857-6
7. Barbier J, Cranswick LMD (2006) J Solid State Chem 179:3958–3964
8. Zou WG, Lu MK, Gu F, Xiu ZL, Wang SF, Zhou GJ (2006) Opt Mater 28:988–991
9. Kim HG, Kang JK, Lee SH, Chung SJ (1998) J Cryst Growth 187:455–462
10. Penin N, Seguin L, Touboul M, Nowogrocki G (2001) Int J Inorg Mater 3:1015–1023
11. Pushcharovsky DY, Gobetchia ER, Pasero M, Merlino S, Dimitrova OV (2002) J Alloys Compd 339:70–75
12. Pan SL, Wu YC, Fu FZ, Zhang GC, Wang GF, Guan XG, Chen CT (2002) J Cryst Growth 236:613–616
13. Li J, Wang JY, Cheng XF, Hu XB, Wang XQ, Zhao SR (2004) Mater Lett 58:1096–1099
14. Prabha K, Kumar TR, Du SF, Vimalan M, Dayalan A, Sagayaraj P (2010) Mater Chem Phys 121:22–27
15. Jiao ZW, Zhang F, Yan QF, Shen DZ, Shen GQ (2009) J Solid State Chem 182:3063–3066
16. Chen AM, Xu SF, Ni ZM (2009) Acta Phys Chim Sin 25:2570–2574
17. Li J, Xia SP, Gao SY (1994) Spectrochim Acta 4:519–532
18. Wang YF, Liu JJ, Hu SF, Lan GX (1999) Chin J Light Scatt 11:87–95
19. Kasprowicz D, Runka T, Szybowicz M, Ziobrowski P, Majchrowski A, Michalski E, Drozdowski M (2005) Cryst Res Technol 4:459–465